Multinuclear Magnetic Resonance Studies of the 2Fe·2S* Ferredoxin from *Anabaena* Species Strain PCC 7120. 3. Detection and Characterization of Hyperfine-Shifted Nitrogen-15 and Hydrogen-1 Resonances of the Oxidized Form†

Byung-Ha Oh and John L. Markley*

Department of Biochemistry, College of Agricultural and Life Sciences, University of Wisconsin—Madison, 420 Henry Mall, Madison, Wisconsin 53706

Received October 19, 1989; Revised Manuscript Received December 28, 1989

ABSTRACT: All the nitrogen signals from the amino acid side chains and 80 of the total of 98 backbone nitrogen signals of the oxidized form of the 2Fe·2S* ferredoxin from *Anabaena* sp. strain PCC 7120 were assigned by means of a series of heteronuclear two-dimensional experiments [Oh, B.-H., Mooberry, E. S., & Markley, J. L. (1990) *Biochemistry* (second paper of three in this issue)]. Two additional nitrogen signals were observed in the one-dimensional ^{15}N NMR spectrum and classified as backbone amide resonances from residues whose proton resonances experience paramagnetic broadening. The one-dimensional ^{15}N NMR spectrum shows nine resonances that are hyperfine shifted and broadened. From this inventory of diamagnetic nitrogen signals and the available X-ray coordinates of a related ferredoxin [Tsukihara, T., Fukuyama, K., Nakamura, M., Katsube, Y., Tanaka, N., Kakudo, M., Wada, K., Hase, T., & Matsubara, H. (1981) *J. Biochem. 90*, 1763–1773], the resolved hyperfine-shifted ^{15}N peaks were attributed to backbone amide nitrogens of the nine amino acids that share electrons with the 2Fe·2S* center or to backbone amide nitrogens of two other amino acids that are close to the 2Fe·2S* center. The seven ^{15}N signals that are missing and unaccounted for probably are buried under the envelope of amide signals. ^1H NMR signals from all the amide protons directly bonded to the seven missing and nine hyperfine-shifted nitrogens were too broad to be resolved in conventional 2D NMR spectra. From their dependence on the magnetogyric ratio, a ^1H resonance should be up to 100 times broader than a ^{15}N resonance that experiences a similar hyperfine interaction. This appears to be the reason why more well-resolved hyperfine-shifted ^{15}N resonances were observed than corresponding ^1H resonances. The results suggest that hyperfine-shifted ^{15}N peaks can provide a unique window on the electronic structure and environment of this and other paramagnetic centers.

The ^1H NMR[1] spectra of plant-type ferredoxins, in both the oxidized and reduced forms of the protein, have been found to exhibit a number of broad resonances whose chemical shifts normally are temperature dependent and lie outside the normal diamagnetic region (0–10 ppm). Resonances of this kind arise from the interaction of nuclear spins with unpaired electron spins through chemical bonds (contact mechanism) and/or through space (pseudocontact mechanism). Such hyperfine interactions produce internal magnetic fields at the resonating nuclei that either add to or subtract from the external magnetic field (Webb, 1970). Hyperfine-shifted ^1H NMR peaks have been reported for spinach and parsley ferredoxins (Poe et al., 1971) and for the ferredoxin I from the cyanobacterium *Anabaena variabilis* (Chan & Markley, 1983a).

With the reduced form of these ferredoxins, eight hyperfine-shifted resonances consistently have been detected by ^1H NMR in the chemical shift range −5 to 45 ppm; these have been assigned to $^1H^{\alpha}$ and/or $^1H^{\beta}$ atoms of the four cysteine ligands. Bertini et al. (1984) observed three additional hyperfine-shifted ^1H resonances in the 60-MHz ^1H NMR spectrum at around 100–140 ppm. Skjeldal et al. (1990) found that these signals are resolved progressively into four resonances in 400, 500, and 600 MHz. The total of 12 resonances account for all the α- and β-protons of four ligated cysteines.

Fewer resolved hyperfine-shifted ^1H resonances have been found with oxidized ferredoxins than with reduced ferredoxins. Poe et al. (1971) found a single hyperfine-shifted peak at about 14.5 ppm in the 220-MHz ^1H NMR spectrum of oxidized spinach and parsley ferredoxins. Salmeen and Palmer (1972) observed a broad envelope of aggregate intensity 6 ± 2 protons at 34–37 ppm in the 60-MHz ^1H NMR spectrum of oxidized spinach ferredoxin; they assigned these peaks speculatively to $^1H^{\beta}$'s of the four cysteine ligands. The assignment was based solely on the observation that the intensity of the envelope accounts for approximately eight protons. Later, it was found that the same signals can be observed at higher magnetic fields: at 200 MHz in ^1H NMR spectra of ferredoxins from spinach and the red alga *Porphyra umbilicalis* (Banci et al., 1990), at 400 MHz (see Figure 2, below), and even at 600 MHz in spectra of *Anabaena* 7120 ferredoxin (Skjeldal et al., 1990).

†Supported by USDA Competitive Grants 85-CRCR-1-1589 and 88-37262-3406. This study made use of the National Magnetic Resonance Facility at Madison, which is supported in part by NIH Grant RR023021 from the Biomedical Research Technology Program, Division of Research Resources. Equipment in the facility was purchased with funds from the University of Wisconsin, the NSF Biological Biomedical Research Technology Program (Grant PR023021), the NIH Shared Instrumentation Program (Grant PR02781), and the U.S. Department of Agriculture. B.-H.O. is supported by a Peterson Fellowship from the University of Wisconsin—Madison.

* To whom correspondence should be addressed.

[1] Abbreviations: a_N, hyperfine coupling constant; β, Bohr magneton; γ_e, magnetogyric ratio of the electron; γ_N, magnetogyric ratio of the nucleus; g, electronic g value of the paramagnetic center; $\mathbf{g}_{\parallel}$, $\mathbf{g}$ tensor parallel to the symmetry axis; $\mathbf{g}_{\perp}$, $\mathbf{g}$ tensor perpendicular to the symmetry axis; H_o, magnetic field strength; ΔH_{hc}, isotropic contact resonance shift; ΔH_{pc}, pseudocontact resonance shift; k, Boltzmann constant; NMR, nuclear magnetic resonance; S, total electron spin quantum number; T_1, spin–lattice relaxation time; T_e, electron spin relaxation time; θ, angle between the distance vector and the symmetry axis; τ_r, rotational correlation time; τ_c, effective correlation time; TSP, (trimethylsilyl)-propionate.

0006-2960/90/0429-4012$02.50/0

Banci et al. (1990) assigned these signals to the $^{1}H^{\beta}$'s of four cysteine ligands by theoretical calculation. This assignment has been confirmed indirectly by the observation of nearly the same signals at 38 ppm in the ^{1}H NMR spectrum of bis[(*o*-xylenedithiolato)(μ_2-sulfido)ferrate(III)], an analogue of the 2Fe·2S* center (Mayerle et al., 1973).

Chan and Markley (1983a) resolved and determined the temperature dependence of hyperfine-shifted ^{13}C resonances of *A. variabilis* ferredoxin I. They observed 11 hyperfine-shifted ^{13}C resonances in the spectrum of the reduced ferredoxin I but only two broad peaks at around 75 and 168 ppm in that of the oxidized ferredoxin I. None of the hyperfine-shifted ^{13}C resonances were assigned to specific amino acids.

Since the electron spin relaxation time of the 2Fe·2S* center is longer in oxidized ferredoxin than in reduced ferredoxin (Wishnia, 1960), nuclear spin relaxation times of nuclei close to the 2Fe·2S* center are expected to be shorter in the oxidized state than in the reduced state (Bertini, 1979). This explains why fewer hyperfine-shifted resonances are detected in spectra of oxidized ferredoxin than in spectra of reduced ferredoxin. These unfavorable magnetic properties of oxidized 2Fe·2S* ferredoxins have hindered the observation of ^{1}H and ^{13}C resonances from amino acid residues in the vicinity of the iron–sulfur cluster that may influence the redox potential or be involved in electron-transfer mechanisms. A nucleus with a lower magnetogyric ratio, such as ^{15}N, will be influenced much less by the paramagnetism (Bloembergen & Morgan, 1961) of the iron–sulfur center. Thus, signals should be resolved from nitrogens under conditions where those of adjacent carbons or hydrogens are broadened beyond detection. Despite this expectation, no hyperfine-shifted ^{15}N resonance from any paramagnetic biomolecule has been reported previously. We describe here the detection and characterization of nine hyperfine-shifted ^{15}N peaks from oxidized *Anabaena* 7120 ferredoxin and discuss these in comparison to the hyperfine-shifted ^{1}H peaks of the protein.

Materials and Methods

Materials. Materials used in this study were described in the first and the second papers in this series (Oh & Markley, 1990; Oh et al., 1990).

NMR Spectroscopy. ^{1}H NMR spectra were collected on a Bruker AM-400 wide-bore NMR spectrometer (9.4 T for ^{1}H) with a 5-mm ^{1}H probe. The 90° ^{1}H pulse width was 6 μs. ^{15}N NMR spectra were collected on a Bruker AM-500 NMR spectrometer with a 5-mm broad-band probe; WALTZ ^{1}H decoupling (Shaka et al., 1983) was employed during acquisition to collapse ^{1}H–^{15}N couplings. The conventional 180°–τ(delay)–90° pulse sequence (Vold et al., 1968), with the 180° pulse replaced by a composite 90°–180°–90° pulse (Freeman et al., 1980), was used for the ^{15}N T_1 relaxation study. Temperature studies of hyperfine-shifted ^{15}N resonances were carried out on a Bruker, AM-400 wide-bore NMR spectrometer with a 10-mm broad-band probe without ^{1}H decoupling. For temperatures below 20 °C, dry air was passed through a cooling unit (FTS Systems, Inc., Model XR-85-1) with a temperature controller (FTS Systems, Inc., Model TC-44) and then into the NMR probe.

^{1}H chemical shifts are referenced to internal TSP. ^{15}N chemical shifts are referenced to liquid ammonia; the resonance of [^{15}N]ammonium sulfate used as the external standard was assumed to be 21.6 ppm at 25 °C.

Results and Discussion

Hyperfine-Shifted ^{15}N Resonances. The 1D ^{15}N NMR spectrum of oxidized ferredoxin (Figure 1, bottom) shows nine

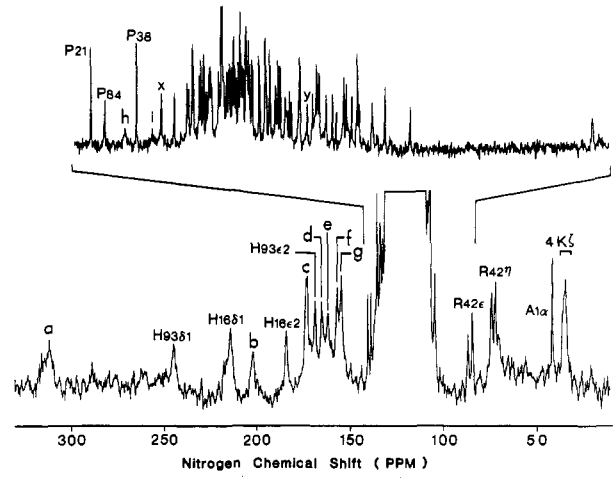

FIGURE 1: One-dimensional ^{15}N NMR spectra of oxidized *Anabaena* 7120 ferredoxin. Hyperfine-shifted resonances are labeled with lowercase letters (a–i). (Top) Proton-decoupled ^{15}N spectrum (50.68 MHz) of 6.5 mM [98% U-^{15}N]ferredoxin in 0.5 mL of 50 mM phosphate buffer containing 90% $^{1}H_2O$/10% $^{2}H_2O$ at pH 7.1. 10000 transients were collected as 16K data points over 411 ppm; the total recycling time was 6.39 s. WALTZ-16 ^{1}H decoupling (Shaka et al., 1983) was carried out during acquisition to collapse ^{1}H–^{15}N coupling. No line broadening (LB) was applied to the FID. Only the region containing amide and arginine side-chain nitrogen resonances is shown. The hyperfine-shifted signal labeled i becomes more apparent when spectral sensitivity is enhanced (see Figure 3). Peak x appears to be relatively normal, but its directly bonded $^{1}H^{N}$ and $^{13}C'$ are broadened by hyperfine interactions (see Discussion). Peak y locates the ^{15}N resonance that corresponds to the cross peak indicated by a rectangle in the $^{1}H\{^{15}N\}$ SBC spectrum (Oh et al., 1990; Figure 4). (Bottom) Proton-coupled 40.55-MHz ^{15}N spectrum of 1.48 mM [98% U-^{15}N]ferredoxin in 2.2 mL of 40 mM phosphate buffer containing 90% $^{1}H_2O$/10% $^{2}H_2O$ at pH 7.1 and 15 °C. A line broadening of 20 Hz was applied to the FID to enhance spectral sensitivity. A total of 40000 transients were collected as 32K data points over 500 ppm; the recycling time was 0.82 s. The line width of peak a increased with increasing sample temperature, probably as the result of a minor thermal perturbation of the protein structure.

broad signals (peaks a–i) that lie downfield of the normal amide nitrogen region and are attributed (see below) to ^{15}N atoms that are close enough to the paramagnetic 2Fe·2S* center to experience hyperfine interactions. From the sequence of the ferredoxin (Alam et al., 1986), the total nitrogen count is 97 backbone amide nitrogens, one amino-terminal nitrogen, and 17 side-chain nitrogens [from 1 Asn (1), 1 Arg (3), 2 His (4), 4 Lys (4), and 5 Gln (5)]. Since the diamagnetic nitrogen assignments (Oh et al., 1990) account for all expected ^{15}N resonances from the amino terminus and side chains, we can conclude that the nine observed hyperfine-shifted ^{15}N signals must arise from peptide backbone nitrogens, all shifted downfield.

Sequence-specific assignments were determined for 76 of the 98 amide nitrogen signals (Oh et al., 1990). An additional amide nitrogen was counted in the $^{1}H\{^{15}N\}$ SBC spectrum but not assigned (Oh et al., 1990; Figure 4, marked by a rectangle); the ^{15}N resonance of this amide is labeled "y" in the 1D ^{15}N spectrum (Figure 1, top). Resonances from all three prolines and from the N-terminal nitrogen were observed at their normal spectral positions and assigned specifically (Figure 1, top). Thus, a total of 81 diamagnetic backbone nitrogens were counted by virtue of the resolving power of the 2D NMR experiments. An additional nitrogen identified in the diamagnetic region of the 1D ^{15}N NMR spectrum labeled "x" Figure 1, top) did not exhibit a cross peak in either the $^{1}H\{^{15}N\}$ SBC or $^{13}C\{^{15}N\}$ SBC spectrum. This suggests that, although the nitrogen has a normal line width and nearly typical amide chemical shift, the attached $^{1}H^{N}$ and the $^{13}C'$ of the previous

residue are broadened by hyperfine interactions. Thus, of the 98 backbone nitrogen signals expected on the basis of the protein sequence, a total of seven were missing and 91 were resolved (82 "normal" and 9 "perturbed").

None of the observed hyperfine-shifted ^{15}N resonances showed a cross peak in the $^{1}H\{^{15}N\}$ SBC spectrum (Oh et al., 1990; Figure 7). The line widths of the hypefine-shifted ^{15}N resonances themselves cannot explain the absence of these cross peaks, because histidine ring nitrogens with equivalent line widths showed cross peaks resulting from 10-Hz coupling in an experiment that was optimized for 90-Hz coupling. Thus, the signals from the hydrogens attached to the hyperfine-shifted nitrogens must be broadened in excess of the amide $^{1}H-^{15}N$ coupling constant ($^{1}J_{NH}$ = 90 Hz).

The amino acid residues that share electrons directly with the 2Fe·2S* center are the four cysteine ligands plus those residues (Ser[40], Ala[43], Gly[44], Ala[45], Thr[48]) reported to make NH···S hydrogen bonds to the 2Fe·2S* center (also OH···S in the case of Ser[40]) (Tsukihara et al., 1986). We designate these amino acids as "class I". Nuclei of class I residues are expected to experience contact interactions (through covalent or hydrogen bonds) as well as pseudocontact interactions (through space). We designate as "class II" the other amino acid residues whose spin systems were not observed or were only partially observed in 2D NMR spectra (Phe[39], Arg[42], Ser[47], Ala[50], Phe[66], Leu[78], Thr[79], and Val[81]).[2] Nuclei of these residues do not share electrons from the 2Fe·2S* center and thus will experience pseudocontact shifts only. Class I amino acids are expected to be more severely perturbed by the paramagnetism than class II amino acids.

Hyperfine-Shifted ^{1}H Resonances. Salmeen and Palmer (1972) and Banci et al. (1990) assigned the broad envelope of peaks at 34–48 ppm observed in ^{1}H spectra recorded in $^{2}H_2O$ to the $^{1}H^{\beta}$'s of the cysteines that ligate the iron–sulfur cluster. In accordance with this assignment, we expect that ^{1}H signals from class II residues should be broadened and shifted much less than these observed class I signals. Nevertheless, the only other hyperfine-shifted ^{1}H resonance we could detect outside the diamagnetic envelope of the oxidized ferredoxin recorded in $^{1}H_2O$ (Figure 2) was the previously observed peak at 14.5 ppm (Poe et al., 1971; Banci et al., 1990).

A reasonable explanation for our failure to observe more ^{1}H resonances from class I and II amino acids is that they are buried in the diamagnetic region of the spectrum and that their line widths, while narrower than the observed hyperfine-shifted resonances, are too broad to be detected in conventional 2D NMR spectra. In less-crowded regions of the diamagnetic envelope, we identified two such peaks [labeled with an asterisk (*) in Figure 2]. Inversion–recovery T_1 measurements showed that these resonances relax faster than the other signals (data not shown).

No solvent-exchangeable hyperfine-shifted peaks were detected in ^{1}H NMR spectra of the oxidized ferredoxin. Apparently, NH···S-type hydrogen bonds are too weak to give rise to contact shifts that are large enough to displace the resonances beyond the diamagnetic envelope.

Paramagnetic Effect on ^{15}N Resonances. The line widths of nuclei experiencing pseudocontact interactions are proportional to the square of the magnetogyric ratio γ (Bloembergen & Morgan, 1961). Since $\gamma_{^{1}H}$ is about 10 times that of $\gamma_{^{15}N}$, the pseudocontact broadening experienced by a ^{1}H nucleus should be 100 times that of a ^{15}N nucleus at the same distance from the paramagnetic center. Thus, hyperfine-shifted ^{15}N resonances should be far better resolved than hyperfine-shifted ^{1}H resonances. Considering the distances between the nuclei and the paramagnetic center, the $^{1}H^{\beta}$'s of cysteinyl ligands should be more perturbed than any nitrogen atoms in the ferredoxin. Since cysteine $^{1}H^{\beta}$ resonances can be observed in the 1D ^{1}H NMR spectrum, the ^{15}N resonances of all class I and class II nitrogen atoms should be observable in 1D ^{15}N NMR spectra. Thus, the observed nine broad hyperfine-shifted ^{15}N peaks likely correspond to the amide nitrogens of the nine class I amino acids (four cysteines and five other amino acids involved in NH···S hydrogen bonds to the iron–sulfur cluster). The missing seven ^{15}N resonances then should correspond to amide nitrogens of seven of the eight class II amino acids. They may be broadened but are not shifted, and they are not observed in $^{1}H-^{15}N$ correlated 2D spectra because of the broadening of the amide protons (line widths > 90 Hz).

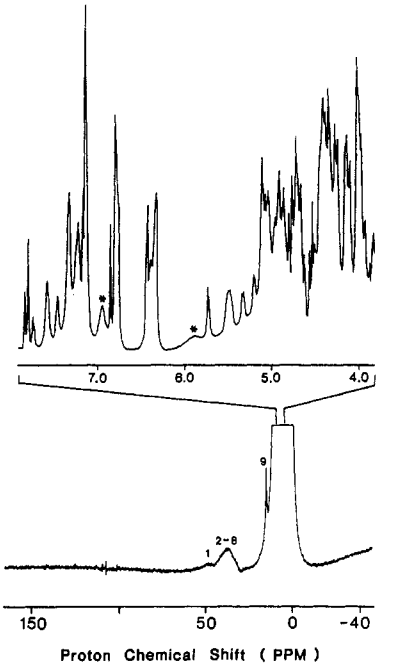

FIGURE 2: 1D ^{1}H NMR spectra (400.13 MHz) of oxidized *Anabaena* 7120 ferredoxin obtained with different spectral widths. The sample consisted of 6.5 mM ferredoxin in 0.5 mL of 50 mM phosphate buffer at 25 °C. (Top) A total of 180 transients were collected as 8K data points over 14 ppm. The asterisks indicate resonances that are two broad to appear in conventional 2D NMR spectra. The spectrum was recorded in $^{2}H_2O$; the pH* of the sample was 7.5. (Bottom) A total of 2000 transients were collected as 16K data points over 340 ppm. The peaks in the region 34–48 ppm were observed previously as a single broad envelope at low magnetic field (Salmeen & Palmer, 1972). At the higher field used here, the resonances are separated into two regions; peak 1 at 48 ppm and peaks 2–8 at 34–38 ppm. The spectrum was recorded in 90% $^{1}H_2O$/10% $^{2}H_2O$; the pH of the sample was 7.1. Solvent suppression was achieved by irradiation at the solvent frequency during the relaxation delay (1.2 s).

Since the iron–sulfur center contains two iron atoms, nuclear relaxation times, considering only electron–nucleus dipolar interaction (pseudocontact interaction), are given by (Bloembergen et al., 1948)

$$\frac{1}{T_1} = \frac{4S(S+1)(g^2\beta^2\gamma_N^2)}{3d_1^6}\tau_c + \frac{4S(S+1)(g^2\beta^2\gamma_N^2)}{3d_2^6}\tau_c \quad (1)$$

where d_1 and d_2 are the distances between the resonating nucleus and Fe^1 and Fe^2, respectively. Fe^1 is defined as the iron atom that is ligated to Cys[41] and Cys[46]; Fe^2 is defined as

[2] The amide proton signal from Ser[65] appears to have been obliterated by water irradiation rather than paramagnetic perturbation (Oh & Markley, 1990). It is not included in this list.

Table I: Distances (Å) between Two Iron Atoms of the 2Fe-2S* Center and the Backbone Nitrogens of Class I and Class II Amino Acids plus N^{ϵ} of Arg^{42} and N of Pro^{38} and Ser^{65}

class I[a]				class II[a] (plus Pro^{38} and Ser^{65})			
residue nitrogen	distance from Fe^{1}[b]	distance from Fe^{2}	reduced distance[c]	residue nitrogen	distance from Fe^{1}	distance from Fe^{2}	reduced distance
Cys^{41}(N)	3.72	5.80	4.13	Arg^{42}(N)	3.44	4.57	3.76
Ser^{40}(N)	4.00	5.29	4.36	Ser^{47}(N)	5.00	5.44	5.19
Cys^{46}(N)	4.24	5.40	4.60	Ala^{50}(N)	7.44	5.66	6.17
Ala^{43}(N)	4.71	4.92	4.80	Phe^{39}(N)[d]	6.32	6.35	6.34
Cys^{49}(N)	5.60	4.62	4.95	Arg^{42}(N^{ϵ})	6.28	6.63	6.44
Gly^{44}(N)	5.18	4.82	4.98	Thr^{79}(N)	9.02	6.48	7.12
Ala^{45}(N)	5.19	5.87	5.46	Val^{81}(N)	8.77	6.63	7.23
Thr^{48}(N)	5.42	5.57	5.49	Leu^{78}(N)	10.37	7.90	8.01
Cys^{80}(N)	7.57	5.16	5.70	Pro^{38}(N)	9.33	8.81	9.04
				Phe^{66}(N)	11.12	9.32	9.96
				Ser^{65}(N)	13.61	11.76	12.46

[a] See text for the definition of class I and II. [b] Distances were calculated from the coordinates of *Spirulina platensis* ferredoxin (Tsukihara et al., 1981). [c] The reduced distance (d_r) is defined in the text. [d] Residue 39 in *S. platensis* ferredoxin is tyrosine; it is replaced by phenylalanine in *Anabaena* 7120 ferredoxin. The distances of the nitrogen from the iron atoms are assumed to be identical in both proteins.

the iron atom that is ligated to Cys^{49} and Cys^{80}. The effective correlation time τ_c is given by

$$1/\tau_c = 1/T_e + 1/\tau_r \quad (2)$$

where T_e is the electronic T_1 and τ_r is the rotational correlation time. Since the T_e for high-spin Fe(III) at room temperature was measured as 10^{-10}–10^{-11} s (Wishnia, 1960), the $1/\tau_r$ term can be neglected for proteins.

By assuming that the g value is the same for two irons (both are ferric [Fe(III)] in the oxidized protein), eq 1 can be reduced to

$$\frac{1}{T_1} + \frac{4S(S+1)(g^2\beta^2\gamma_N^2)}{3d_r^6}\tau_c \quad (3)$$

where d_r is $[2d_1^6d_2^6/(d_1^6 + d_2^6)]^{1/6}$. Thus, a nucleus at distances of d_1 and d_2 from Fe^1 and Fe^2, respectively, would be affected the same as a hypothetical nucleus equidistant (d_r) from both iron atoms.

In the inversion–recovery T_1 measurement study (Figure 3), the three assigned proline ^{15}N signals relaxed more slowly than any other ^{15}N signals in the diamagnetic region. This reflects the fact that the predominant relaxation mechanism for a diamagnetic backbone amide nitrogen is dipole–dipole interaction with its attached proton; the proline nitrogen does not have an attached proton. Since the proline closest to the iron atoms (Pro^{33}, N^{α} d_r = 9.04 Å) had virtually the same relaxation time as those farther away, electron–nitrogen relaxation at this distance is negligible. Thus, any nitrogen nucleus farther than 9.04 Å from the two iron atoms should not be perturbed. Table I shows d_r calculated for the nitrogen atoms whose signals were not assigned by 2D NMR experiments. From Table I, Ser^{65} and Phe^{66}, each of whose nitrogen is more distant from the two irons than that of Pro^{33} (d_r = 9.04 Å), can be excluded as possible candidates for the hyperfine-shifted ^{15}N resonances. A computer-assisted search of the nitrogen atoms within d_r of 9.04 Å of the two irons yielded no amino acid that had been assigned from 2D NMR experiments (Oh et al., 1990) with the exception of the N^{ϵ} of Arg^{42} (d_r = 6.44 Å), which was observed at its normal chemical shift position (Figure 1, top). Its longitudinal relaxation rate is comparable to diamagnetic ^{15}N signals. If we assume that the position of the Arg^{42} side chain is the same in solution as it is in the crystal of the related ferredoxin, then we can impose a more stringent distant constraint. In applying the distance constraint, $d_r < 6.44$ Å, the nitrogens of Thr^{79}, Val^{81}, and Leu^{78} (class II amino acids) are excluded. Ala^{50} and Phe^{39} (d_r = 6.17 and 6.34 Å, respectively) also can be excluded since a 0.27-Å shorter distance would not lead to the rapid relaxation observed for the hyperfine-shifted resonances. This reduces the possible candidates to nine class I amino acids and two class II amino acids (Arg^{42}, Ser^{47}). No further constraints are available since no nitrogen closer than d_r = 6.44 Å in the X-ray structure gave a resolved signal. All nitrogens having $d_r \geq 6.44$ Å are expected to have line widths similar

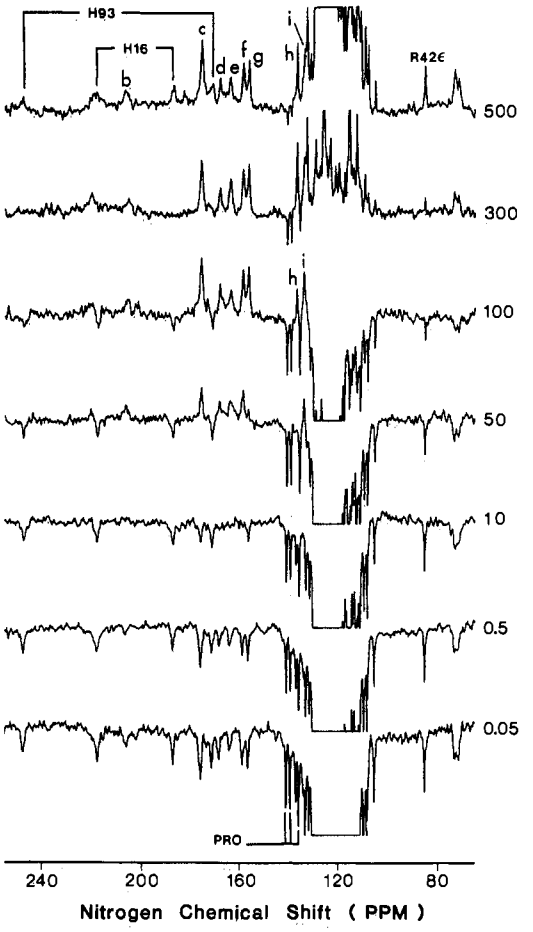

FIGURE 3: ^{15}N NMR relaxation study (50.68 MHz) of oxidized *Anabaena* 7120 [98% U-^{15}N]ferredoxin. The spectra were obtained with a composite pulse (180°–τ–90°) pulse sequence. Sample conditions were as described in Figure 1, top. A total of 11 000 transients were collected as 8K data points over 330 ppm; WALTZ-16 ^{1}H decoupling (Shaka et al., 1983) was carried out during acquisition to collapse ^{1}H–^{15}N coupling. The recycling time was 3.4 s. A line broadening of 20 Hz was applied to the FID. At 25 °C and at this magnetic field strength, hyperfine-shifted peak a was barely visible. The τ values (ms) are given at the end of each trace.

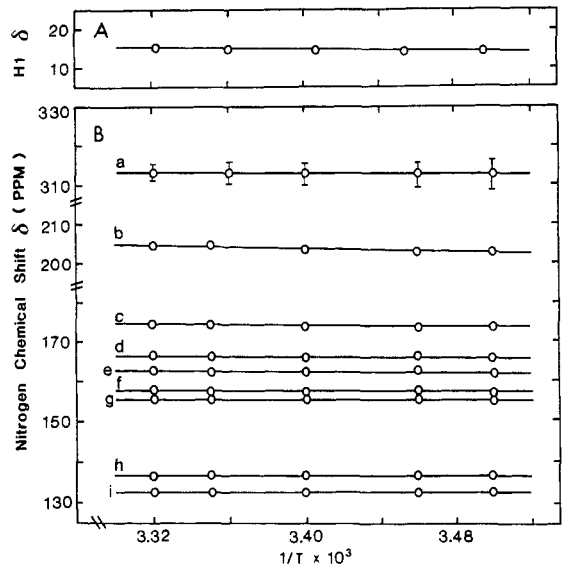

FIGURE 4: Temperature dependence of hyperfine-shifted resonances of oxidized *Anabaena* 7120 ferredoxin: (A) hyperfine-shifted ^{1}H peak at 14.5 ppm observed in the 400-MHz ^{1}H spectrum; (B) nine hyperfine-shifted ^{15}N resonances (measured at 40.55 MHz and labeled as in Figure 1, bottom).

to diamagnetic ^{15}N resonances. The six nitrogens with $d_r \geq 6.44$ Å listed in Table I apparently were not detected in conventional 2D NMR experiments because their attached ^{1}H and ^{13}C are broadened. Resonances x and y in the 1D ^{15}N spectrum (Figure 1, top) probably correspond to two nitrogens in this set.

We studied the temperature dependence of the hyperfine-shifted ^{15}N and ^{1}H resonances in the range of 14–29 °C. Figure 4 is a plot of the chemical shifts of those peaks as a function of the reciprocal of the temperature. Of these hyperfine-shifted peaks, only ^{15}N peak b and the 14.5 ppm ^{1}H peak showed appreciable temperature dependence: 0.3 and 0.2 ppm/°C, respectively. No negative temperature dependence has been observed for any of the hyperfine-shifted ^{1}H (Skjeldal et al., 1990), ^{13}C (Chan & Markley, 1983a), or ^{15}N resonances of oxidized plant-type ferredoxins.

Class II resonances are affected by pseudocontact interactions whose line broadening effect falls off as $1/d^6$ and whose shift effect falls off as $1/d^3$, where d is the separation between the paramagnetic center and the resonating nucleus (Phillips & Poe, 1973). Thus, it is reasonable to expect that some of the NMR signals from class II residues will be shifted but not broadened appreciably. Contrary to this, all the observed hyperfine-shifted ^{1}H, ^{13}C (Chan et al., 1983b), and ^{15}N signals are broadened as well as shifted. The magnitude of the pseudocontact shift is given (McConnell & Robertson, 1958) by

$$\frac{\Delta H_{pc}}{H_o} = -(3\cos^2\theta - 1)(\mathbf{g}_\parallel - \mathbf{g}_\perp)(\mathbf{g}_\parallel + 2\mathbf{g}_\perp)\frac{\beta^2 S(S+1)}{27kTd^3} \quad (4)$$

This appears to indicate that $\mathbf{g}_\parallel$ and $\mathbf{g}_\perp$ in oxidized plant-type ferredoxin are very similar and that all observed hyperfine shifts are contact in origin. However, since the magnitude of the shift is also dependent on the angle θ, one cannot rule out the less likely possibility that $\mathbf{g}_\parallel$ and $\mathbf{g}_\perp$ are different but that no nucleus in the protein is placed such that it gives rise to a large shift.

Some of the observed ^{15}N hyperfine-shifts are quite large compared with the observed ^{1}H hyperfine shifts. If the largest diamagnetic chemical shift of the amide nitrogen is assumed to be 130.5 ppm, the chemical shift of the most-downfield resonance of the assigned diamagnetic amino acids (Leu^{53} ^{15}N), the minimum magnitudes of the ^{15}N hyperfine shifts in ppm are 176.9 (peak a), 71.8 (b), 42.2 (c), 35.0 (d), 30.9 (e), 25.9 (f), 23.7 (g), 5.0 (h), and 2.0 (i). If the diamagnetic chemical shift of the cysteine protons is assumed to be 3 ppm, the magnitudes of the ^{1}H hyperfine shifts are between 11.5 and 45 ppm.

The magnitude of the contact shift is given (McConnell and Chesnut, 1958) by

$$\frac{\Delta H_{hc}}{H_o} = -a_N\frac{\gamma_e}{\gamma_N}\frac{g\beta S(S+1)}{3kT} \quad (5)$$

Provided that the contact shift is a main contributor to the observed hyperfine-shifts, only the class I nitrogens can be candidates for hyperfine-shifted ^{15}N peaks. The ^{15}N of each of the four cysteines is four bonds from an iron atom. The ^{15}N of each of the five amino acids involved in the NH···S hydrogen bonds (Tsukihara et al., 1986) is three bonds distant from an iron, but hyperfine coupling is expected to be attenuated strongly by the weak hydrogen bond. Since the contact hyperfine shift is proportional to the hyperfine coupling constant (a_N), the four most strongly hyperfine-shifted nitrogens may correspond to the cysteine residues, and the five more weakly hyperfine-shifted nitrogens may correspond to the NH···S hydrogen bonds, with the magnitudes reflecting their strength.

Full assignments of the ^{1}H and ^{15}N hyperfine-shifted resonances will require the labeling of individual residue types with ^{2}H and ^{15}N. This approach will become possible with heterologous overproduction of the cloned ferredoxin gene product (Alam et al., 1986) in an appropriate host (Böhme & Haselkorn). The labeling of individual residue types with ^{15}N will facilitate the assignment of the observed hyperfine-shifted ^{15}N resonances and permit the detection of the seven undetected ^{15}N signals. It also will be of interest to determine whether hyperfine-shifted nitrogen resonances can be detected in related 2Fe·2S* proteins and in other types of paramagnetic proteins.

ACKNOWLEDGMENTS

We thank Dr. P. Darba for kind help in computer-assisted distance searches and Dr. L. Skjeldal for stimulating discussion.

REFERENCES

Alam, J., Whitaker, R. A., Krogmann, D. W., & Curtis, S. E. (1986) *J. Bacteriol. 168*, 1265–1271.

Banci, L., Bertini, I., & Luchinat, C. (1990) *Struct. Bonding* (in press).

Bertini, I. (1979) in *ESR and NMR of Paramagnetic Species in Biological and Related System* (Bertini, I., & Drago, R., Eds.) pp 201–223, D. Reidel Publishing Co., Boston, MA.

Bertini, I., Lanini, G., & Luchinat, C. (1984) *J. Inorg. Chem. 23*, 2729–2730.

Bloembergen, N., & Morgan, L. O. (1961) *J. Chem. Phys. 34*, 842–850.

Böhme, H., & Haselkorn, R. (1989) *Plant Mol. Biol. 12*, 667–672.

Chan, T.-M., & Markley, J. L. (1983a) *Biochemistry 22*, 6008–6010.

Chan, T.-M., & Markley, J. L. (1983b) *Biochemistry 22*, 5996–6002.

Freeman, R., Kempsell, S. P., & Levitt, M. H. (1980) *J. Magn. Reson. 38*, 453–479.

Mayerle, J. J., Frankel, R. B., Holm, R. H., Ibers, J. A., Phillips, W. D., & Weiher, J. F. (1973) *Proc. Natl. Acad. Sci. U.S.A. 70*, 2429–2433.
McConnell, H. M., & Chesnut, D. B. (1958) *J. Chem. Phys. 28*, 107–117.
McConnell, H. M., & Robertson, R. E. (1958) *J. Chem. Phys. 29*, 1361–1365.
Oh, B.-H., & Markley, J. L. (1990) *Biochemistry* (first paper of three in this issue).
Oh, B.-H., Mooberry, E. S., & Markley, J. L. (1990) *Biochemistry* (second paper of three in this issue).
Phillips, W. D., & Poe, M. (1973) in *Iron Sulfur Proteins* (Lovenberg, W., Ed.) Vol. II, pp 255–284, Academic Press, New York and London.
Poe, M., Phillips, W. D., Glickson, J. D., McDonald, C. C., & San Pietro, A. (1971) *Proc. Natl. Acad. Sci. U.S.A. 68*, 68–71.
Salmeen, I., & Palmer, G. (1972) *Arch. Biochem. Biophys. 150*, 767–773.
Shaka, A. J., Keeler, J., Frenkiel, T., & Freeman, R. (1983) *J. Magn. Reson. 52*, 335–338.
Skjeldal, L., Westler, W. M., & Markley, J. L. (1990) *Arch. Biochem. Biophys.* (in press).
Tsukihara, T., Fukuyama, K., Nakamura, M., Katsube, Y., Tanaka, N., Kakudo, M., Wada, K., Hase, T., & Matsubara, H. (1981) *J. Biochem. 90*, 1763–1773.
Tsukihara, T., Fukuyama, K., & Katsube, Y. (1986) in *Iron-Sulfur Protein Research* (Matsubara, H., et al., Eds.) pp 59–68, Japan Science Society Press, Tokyo.
Vold, R. L., Waugh, J. S., Klein, M. P., & Phelps, D. E. (1968) *J. Chem. Phys. 48*, 3831–3832.
Webb, G. A. (1970) *Annu. Rep. NMR Spectrosc. 3*, 211–259.
Wishnia, A. (1960) *J. Chem. Phys. 32*, 871–875.

Nuclear Magnetic Resonance Study of Sphingomyelin Bilayers

Karol S. Bruzik,* Beata Sobon, and Grzegorz M. Salamonczyk
Center of Molecular and Macromolecular Studies, Polish Academy of Sciences, Sienkiewicza 112, 90-362 Lodz, Poland
Received September 20, 1989; Revised Manuscript Received December 15, 1989

ABSTRACT: Bilayers of D-*erythro*-(*N*-stearoylsphingosyl)-1-phosphocholine (C_{18}-SPM), previously characterized by differential scanning calorimetry [Bruzik, K. S., & Tsai, M.-D. (1987) *Biochemistry 26*, 5364–5368] in various phases, were studied by means of wide-line ^{31}P, ^{2}H, high-resolution ^{13}C CP–MAS, and ^{1}H MAS NMR. The fully relaxed gel phase of C_{18}-SPM at temperatures below 306 K displayed ^{31}P NMR spectra characteristic of the rigid phase with frozen rotation of the phosphocholine head group. Three other gel phases existing in the temperature range 306–318 K displayed spectra with incompletely averaged axially symmetric powder line shapes and were difficult to differentiate on the basis of their ^{31}P NMR spectra. The gel-to-gel transition at 306 K was found to be fully reversible. The main phase transition at 318 K resulted in the formation of the liquid-crystalline phase for which spectra with axially symmetric line shapes of uniform width were obtained, regardless of the nature of the starting gel phase. ^{13}C CP-MAS NMR spectra revealed significant differences in the molecular dynamics of sphingomyelin in various phases. All carbon atoms of the polar head group in the liquid-crystalline phase gave rise to a separate resonance lines. Numerous carbon atom signals were doubled in the stable phase, demonstrating the existence of two slowly interconverting conformers.

The calorimetric phase behavior of bilayers of fully synthetic D-*erythro*-stearoylsphingomyelin [D-*erythro*-C_{18}-SPM, C_{18}-SPM (**1**)] and of its analogues was recently studied in detail

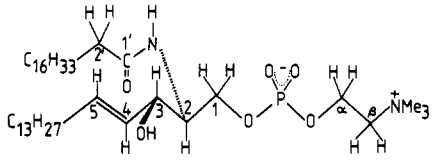

1

(Bruzik & Tsai, 1987; Tsai et al., 1987) and was found to be grossly different from the behavior described for racemic and semisynthetic stearoylsphingomyelin (Barenholz et al., 1976; Barenholz & Thompson, 1980; Estep et al., 1980). However, up to now, the gel and liquid-crystalline phases of pure, synthetic C_{18}-SPM have not been characterized by other techniques. An interesting feature of numerous sphingolipids, including currently described and non-hydroxy fatty acid cerebroside preparations, is that they can form an unusual, highly ordered stable gel phase characterized by the high enthalpy of the gel-to-liquid crystalline phase transition (Ruocco et al., 1981; Curatolo, 1987). The structure of this rigid phase remains unknown, but it has been postulated that it may play a role in biological membranes (Curatolo, 1987; Boggs, 1987). As a possible explanation of the driving force for the formation of such a rigid bilayer phase, the existence of an intermolecular hydrogen bonding network involving an amide function of the ceramide moiety has been proposed (Boggs, 1987; Lee et al., 1986).

In the currently presented work, the properties of sphingomyelin samples equivalent to those described by us earlier were studied by means of multinuclear wide-line and high-resolution NMR spectroscopy.

Materials and Methods

C_{18}-SPM was synthesized and extensively purified as described recently (Bruzik, 1988a; Bruzik & Tsai, 1987). Bovine

* Address correspondence to the author.

0006-2960/90/0429-4017$02.50/0